Journal of Computational and Applied Mathematics 420 (2023) 114841

Contents lists available at ScienceDirect

Journal of Computational and Applied Mathematics

journal homepage: www.elsevier.com/locate/cam

Fitting and filling of 3D datasets with volume constraints using radial basis functions under tension

M.A. Fortes *, P. González, A. Palomares, M. Pasadas

Department of Applied Mathematics, School of Civil Engineering, University of Granada, C/ Severo Ochoa s/n, 18071 Granada, Spain

ARTICLE INFO

Article history:
Received 23 October 2021
Received in revised form 10 September 2022

Keywords:
Radial basis functions
Spline approximation
Hole filling
Smoothing surface
Volume constraints

ABSTRACT

Given a dataset of 3D points in which there is a *hole*, i.e., a region with a lack of information, we develop a method providing a surface that fits the dataset and *fills* the hole. The filling patch is required to fulfill a prescribed volume condition. The fitting–filling function consists of a radial basis functions that minimizes an energy functional involving both, the fitting of the dataset and the volume constraint of the filling patch, as well as the fairness of the function. We give a convergence result and we present some graphical and numerical examples.

1. Introduction

Hole-filling techniques appear in many different real applications, like surface reconstruction in Engineering [1], 3D human body scanning [2], dental reconstruction [3], physics [4], reverse engineering, etc. In 3D scanning applications, for example, data can be missing due to accessibility limitations [5], occlusion, reflecting spaces or surfaces perpendicular to the camera/scanner.

Some papers on this topic deal with methods to fill holes in a given surface by means of variational splines fulfilling different smoothness conditions. For example, in [6] discontinuous and $\mathcal{C}^0$-fillings are proposed, while in [7] the filling considered is $\mathcal{C}^1$. In some practical cases it may be also necessary – due to industrial or design requirements – to impose additional geometric or volumetric constraints on the filling patches (see e.g. [8,9]). In [3] many hole filling algorithms are listed, while in survey [10] the literature on correcting polygonal models of 3D objects is reviewed, including gaps and holes as errors.

Sometimes it is desired that the hole-filling methods, although using limited information, can restore some of the characteristics of the original models [3], as sharp features [1], shape's surfaces defined by derivatives [8], or specific geometric characteristics [11]. In [12] Bézier cubic surfaces are used to interpolate data values and normal directions of tangent planes. Also an iterative method is used by means of a homotopy scheme to minimize a strain energy functional.

In this paper we handle the problem of having a dataset of points (taken, for example, from a given function or from some data acquisition procedure) suffering from a lack of information inside some sub-domains (holes) to which we want to associate a new function over the whole domain that, not only fits the dataset, but also properly *fills* the holes. Notice that technically we do not fill a hole since only some data points from the surface are used. But we think it is not possible to exactly fill the hole of a surface without replacing it by another one approximating it, unless we remove continuity and smoothness conditions on the final global reconstructed fitting–filling surface. We mean, in general it is not possible (neither with RBF nor with splines) that a filling patch interpolates the values of a surface (and the ones of its partial

* Corresponding author.
E-mail addresses: mafortes@ugr.es (M.A. Fortes), prodelas@ugr.es (P. González), anpalom@ugr.es (A. Palomares), mpasadas@ugr.es (M. Pasadas).

https://doi.org/10.1016/j.cam.2022.114841

derivatives if we want additional smoothness) all over the boundary curve of the hole. Therefore, if we want to dispose of a final reconstructed surface being smooth enough, or at least with no discontinuities, it becomes necessary to replace the original surface by another one fitting it. This does not pose a problem since such a fitting surface can be so close to the original one as desired, as stated in the convergence theorem. We want also to mention that, although this paper could have been developed in the general $\mathbb{R}^d$, we have chosen to develop it in the 3D frame since it allows a clearer graphical presentation and interpretation of the results, and it is specially relevant in problems posed in physics and engineering.

Several methods regarding this topic have been developed (see [7,13]) in the literature, but in this work we will make use of an appropriate space of Radial Basis Functions (RBFs), giving both theoretical and computational results that assure the feasibility and good properties of the method proposed: We will look for a function in a vector space, generated by a RBF, minimizing certain quadratic functional including some terms associated with a volume constraint and with the usual semi-norms in a Sobolev space, all of them weighted by *smoothness parameters*. This minimizing functional technique has proved to be effective on some approximation methods in different functional spaces (see [6,14–16] and the references therein). The volume constraint of course will have a clear impact on the filling patch insofar as such a volume strongly affects the shape of the surface. On the other hand, the smoothness parameters can be chosen in such a way that different weights can be given to the different summands of the energy functional (fitting, volume and fairness). A deep study of how these parameters affect the final surface can be carried out by means of the cross-validation method (see for instance [14]).

RBFs have turned out to be a successful technique in the function approximation theory in general. For example, in [5,17], holes are filled by using this kind of functions on the hole neighborhood. In [18], zero-valued surface points and non-zero off-surface points are considered to define a signed-distance function in order to do so. These radial basis techniques have important advantages, like the needless of any mesh or partition in the computational domain – for that reason they are usually called *meshless* methods –, the great flexibility and adaptation to the shape of the data and the amazing simplicity and performance of the related procedures. These advantages lead to very good results even using just a few of such functions, with a reduced computational cost and storage requirements.

This work intends to overcome two problems that arisen in other related papers – mainly using finite elements –: On one hand, handling triangulations fine enough to get fillings of enough quality necessarily implies the use of large linear systems that, moreover, translates into bad-conditioning. More precisely, when using finite elements the dimension of the associated linear systems are of order several times (at least 3 if $\mathcal{C}^1$-fillings are desired) the number of knots in the underlying triangulation. On other hand, using finite element necessarily requires a triangulation of the whole domain and, more specifically, of the hole. When such a hole is not *fair, smooth* enough to be triangulated by a relatively straightforward – and near to uniform – triangulation, additional difficulties arisen as, in this case, either acute triangles or very fine triangulations are needed to properly triangulate the hole, leading to severe computational problems or bad-conditioning, respectively, or even both.

It is also worthy to mention that the proposed method presents a limitation regarding the computation when high dimensions are considered. We mean, given the hole, the dataset and the volume constraint the existence and the uniqueness of the fair function fitting and filling the dataset and fulfilling the volume objective V is guaranteed with no additional requirements. Nevertheless, insofar as the size of the linear system leading to the solution is the dimension of the space where the fitting–filling function is searched for, we will for sure find bad-conditioning as this dimension grows. In particular, the convergence result, which is naturally linked to an infinite grow of the dimension of the space, could not be illustrated by examples. The study of the conditioning of the linear systems associated to this problem could be of course addressed (see e.g. [19]).

The outline of the work is as follows: in Section 2 we introduce some notation and we recall some basic concepts and results that will be used throughout the paper. In Section 3 we present the main problem we want to study, we show the existence and the uniqueness of the solution, and we deal with the computation of the solution. In Section 4 we present a convergence result, for which it will be necessary to previously recall some other results in the literature. In Section 5 we include some graphical and numerical examples to show the performance of the method. The paper ends with a conclusions section.

2. Notation and preliminaries

For any natural number $m \geq 1$, let $\Pi_{m-1}(\mathbb{R}^2)$ denote the space of bivariate polynomials of degree at most $m-1$ defined on $\mathbb{R}^2$, whose dimension is $d(m) = \dfrac{m(m+1)}{2}$, and let $\{q_1, \ldots, q_{d(m)}\}$ be any basis of $\Pi_{m-1}(\mathbb{R}^2)$.

Throughout this paper Ω will denote a nonempty, open, bounded and connected subset of $\mathbb{R}^2$ having Lipschitz boundary.

We will use the notation $\langle\cdot\rangle_n$ to denote the usual Euclidean norm in $\mathbb{R}^n$, and $H^k(\Omega)$ to denote the usual Sobolev space of all distributions whose weak partial derivatives up to order k belong to the classical Lebesgue space $L^2(\Omega)$. It is well known that $H^k(\Omega)$ is a Hilbert space equipped with the linear semi-products

$$(u, v)_\ell = \sum_{|\alpha|=\ell} \int_\Omega D^\alpha u(x) D^\alpha v(x) dx, \quad 0 \leq \ell \leq k,$$

where $\boldsymbol{\alpha} = (\alpha_1, \alpha_2) \in \mathbb{N}^2$, $|\boldsymbol{\alpha}| = \alpha_1 + \alpha_2$, and $D^{\boldsymbol{\alpha}}$ represents the operator $\dfrac{\partial^{|\boldsymbol{\alpha}|}}{\partial x_1^{\alpha_1} \partial x_2^{\alpha_2}}$; the seminorms

$$|u|_\ell = (u, u)_\ell^{\frac{1}{2}}, \quad 0 \le \ell \le k;$$

and the norm $\|u\|_k = \left(\sum_{\ell=0}^{k} |u|_\ell^2 \right)^{\frac{1}{2}}$.

For $X = \Omega$ or $X = \mathbb{R}^2$ let us consider the space

$$X^m(X) = \{u \in \mathcal{D}(X) : D^{\boldsymbol{\alpha}} u \in L^2(X) \text{ for } |\boldsymbol{\alpha}| = m, m+1\},$$

where $\mathcal{D}(X)$ is the space of the Schwartz distributions, endowed with the semi-product

$$(u, v)_{m,\tau,X} = \left(\sum_{|\boldsymbol{\alpha}|=m+1} \frac{(m+1)!}{\boldsymbol{\alpha}!} \int_X (D^{\boldsymbol{\alpha}} u(x))^2 dx + \tau^2 \sum_{|\boldsymbol{\alpha}|=m} \frac{m!}{\boldsymbol{\alpha}!} \int_X (D^{\boldsymbol{\alpha}} u(x))^2 dx \right)^{\frac{1}{2}},$$

where $\boldsymbol{\alpha}! = \alpha_1! \alpha_2!$, and the corresponding seminorm $|u|_{m,\tau,X} = (u, u)_{m,\tau,X}^{\frac{1}{2}}$.

Remark 1. The space $X^m(\mathbb{R}^2)$ equipped with this inner semi-product is a semi-Hilbert space continuously embedded in the space $\mathcal{C}(\mathbb{R}^2)$. The null space of the semi-normed space $(X^m(\mathbb{R}^2), |\cdot|_{m,\tau,\mathbb{R}^2})$ is $\Pi_{m-1}(\mathbb{R}^2)$ (see for example [20]).

Consider the function $\phi_\tau : [0, +\infty) \to \mathbb{R}$ given by

$$\phi_\tau(t) = -\frac{1}{2\tau^3} \left(e^{-\tau\sqrt{t}} + \tau\sqrt{t} \right), \quad t \ge 0, \tag{1}$$

for some $\tau > 0$, whose associated radial function on $\mathbb{R}^2$ is

$$\Phi_\tau(x) = \phi_\tau(\langle x \rangle^2) = -\frac{1}{2\tau^3} \left(e^{-\tau \langle x \rangle_2} + \tau \langle x \rangle_2 \right), \quad x \in \mathbb{R}^2.$$

Remark 2. It holds that $\phi_\tau \in \mathcal{C}([0, +\infty)) \cap \mathcal{C}^\infty(0, \infty)$ and that the function Φ_τ is conditionally strictly positive of order $m \ge 1$ on $\mathbb{R}^2$ (see Theorems 2 and 3 of [21]).

Let $N \in \mathbb{N}$ be such that $N \ge d(m)$; $\mathcal{X} \equiv \mathcal{X}^N = \{x_1, \ldots, x_N\} \subset \overline{\Omega}$ be an arbitrary set containing a $\Pi_{m-1}(\mathbb{R}^2)$-unisolvent subset (i.e., if $q \in \Pi_{m-1}(\mathbb{R}^2)$ satisfies $q(x_i) = 0$ for all $i = 1, \ldots, N$, then $q = 0$) and $\mathcal{H} \equiv \mathcal{H}^N$ be the finite-dimensional subspace of $H^{m+1}(\mathbb{R}^2)$ generated by the functions

$$\{\Phi_\tau(\cdot - x_1), \ldots, \Phi_\tau(\cdot - x_N), q_1, \ldots, q_{d(m)}\}. \tag{2}$$

Let

$$h = \sup_{x \in \Omega} \min_{x_i \in \mathcal{X}} \langle x - x_i \rangle_2 \tag{3}$$

be the fill-distance from $\mathcal{X}$ to Ω.

Remark 3. Taking into account Remark 2 it holds that $\mathcal{H}$ is a finite-dimensional subspace of $H^{m+1}(\mathbb{R}^2) \subset X^m(\mathbb{R}^2)$.

Let $\mathcal{H}_{\tau,m}$ be the semi-Hilbert subspace of $\mathcal{C}(\mathbb{R}^2)$ equipped with the inner semi-product $(\cdot, \cdot)_{\tau,m}$ and its associated semi-norm $|\cdot|_{\tau,m}$, given by [21, Theorem 4].

Theorem 1 (*Theorem 5 of [21]*)**.** *Given a set of real interpolation values $\{f_1, \ldots, f_N\} \subset \mathbb{R}$, there exists one and only one function $s_N \in \mathcal{H}_{\tau,m}$ such that $s_N(x_i) = f_i$, for $i = 1, \ldots, N$, and also it minimizes the semi-norm $|\cdot|_{\tau,m}$. Moreover, this function s_N can be written as*

$$s_N(x) = \sum_{i=1}^{N} \lambda_i \Phi_\tau(x - x_i) + \sum_{j=1}^{d(m)} \beta_j q_j(x), \ x \in \mathbb{R}^2, \tag{4}$$

where the coefficients λ_i, for $i = 1, \ldots, N$, and β_j, for $j = 1, \ldots, d(m)$, are the solution of the linear system

$$\begin{pmatrix} A_\tau & M \\ M^\top & O \end{pmatrix} \begin{pmatrix} \boldsymbol{\lambda} \\ \boldsymbol{\beta} \end{pmatrix} = \begin{pmatrix} \boldsymbol{f} \\ \boldsymbol{0} \end{pmatrix}, \tag{5}$$

with

- $A_\tau = (\Phi_\tau(x_i - x_j))_{1\le i,j\le N}$ *being a* $N \times N$ *matrix,*
- $M = (q_j(x_i))_{\substack{1\le i\le N \\ 1\le j\le d(m)}}$ *being a* $N \times d(m)$ *matrix and* $M^\top$ *denoting the transpose of the matrix* M*,*
- O *is the* $d(m) \times d(m)$ *zero matrix,*
- $\boldsymbol{\lambda} = (\lambda_1, \ldots, \lambda_N)^\top$, $\boldsymbol{f} = (f_1, \ldots, f_N)^\top$, $\boldsymbol{\beta} = (\beta_1, \ldots, \beta_{d(m)})^\top$ *and*
- $\mathbf{0}$ *is the zero vector of* $\mathbb{R}^{d(m)}$.

Definition 1. The function $s_N \in \mathcal{H}$ given by (4) and the explicit surface given by its graph are called, respectively, the *interpolation spline under tension* and the *interpolation surface under tension* associated with $\mathcal{X}^N$, $\boldsymbol{f}$, m and τ.

3. Formulation of the problem

Let H (the hole) be an open and nonempty subset of Ω. Let us consider an arbitrary set of points $\mathcal{A} \equiv \mathcal{A}_M = \{a_1, \ldots, a_M\} \subset \Omega - H$ containing a $\Pi_{m-1}(\mathbb{R}^2)$-unisolvent subset. Let us consider the volume objective $V \in \mathbb{R}$; a set of real fitting data $\mathcal{Z} = \{z_1, \ldots, z_M\}$; a vector of smoothing parameters $\boldsymbol{\lambda} = (\lambda_0, \ldots, \lambda_m) \in \mathbb{R}^{m+1}$, with $\lambda_0, \ldots, \lambda_{m-1} \ge 0$ and $\lambda_m > 0$; the evaluation operator

$$\rho : H^m(\Omega) \longrightarrow \mathbb{R}^M$$

given by $\rho(v) = (v(a_i))_{i=1}^M$; and the functional

$$\mathcal{J} : H^m(\Omega) \longrightarrow \mathbb{R}$$

defined by

$$\mathcal{J}(v) = < \rho(v) - \mathcal{Z} >_M^2 + \lambda_0 \left(\int_H v(x)dx - V \right)^2 + \sum_{i=1}^m \lambda_i |v|_i^2. \tag{6}$$

Observe that the first term of $\mathcal{J}$ measures how well (in the least squares sense) v approximates the vector values $\mathcal{Z}$ over the set $\mathcal{A}$, the second one measures how well the signed-volume of v approximates the value V over H, and the last one represents a kind of 'minimal energy condition' over the semi-norms $|\cdot|_i$, $i = 1, \ldots, m$, weighted by the smoothing parameter vector $\boldsymbol{\lambda}$.

The problem we want to solve is:

Problem 1. Find $\sigma \in \mathcal{H}$ such that $\mathcal{J}(\sigma) \le \mathcal{J}(v)$ for all $v \in \mathcal{H}$.

Theorem 2. *Problem 1 has a unique solution which is also the solution of the following variational problem:*

$$\begin{cases} \text{Find } \sigma \in \mathcal{H} \text{ such that} \\ \langle \rho(\sigma), \rho(v) \rangle_M + \lambda_0 \displaystyle\int_H \sigma(x)dx \int_H v(x)dx + \sum_{i=1}^m \lambda_i(\sigma, v)_i = \\ \langle \mathcal{Z}, \rho(v) \rangle_M + \lambda_0 V \displaystyle\int_H v(x)dx, \quad \text{for all } v \in \mathcal{H}. \end{cases} \tag{7}$$

Proof. The map $[[\cdot]]$ defined by

$$[[v]] = \left(\langle \rho(v) \rangle_M^2 + \lambda_0 \left(\int_H v(x)dx \right)^2 + \sum_{i=1}^m \lambda_i |v|_i^2 \right)^{\frac{1}{2}}$$

defines a norm in $\mathcal{H}$ equivalent to the usual norm $\|\cdot\|_m$. Hence, the application $a : \mathcal{H} \times \mathcal{H} \longrightarrow \mathbb{R}$ defined by

$$a(u, v) = \langle \rho(u), \rho(v) \rangle_M + \lambda_0 \int_H u(x)dx \int_H v(x)dx + \sum_{i=1}^m \lambda_i(u, v)_i$$

is a bilinear, continuous, symmetric and $\mathcal{H}$-elliptic form. On the other hand, the map $\Psi : \mathcal{H} \longrightarrow \mathbb{R}$ given by

$$\Psi(v) = \langle \mathcal{Z}, \rho(v) \rangle_M + \lambda_0 V \int_H v(x)dx$$

is a linear and continuous application. Hence, by applying the Lax–Milgram Lemma, we obtain that there exists a unique $\sigma \in \mathcal{H}$ such that $a(\sigma, v) = \Psi(v)$ for all $v \in \mathcal{H}$, which is equivalent to (7). Moreover, σ is the minimum of the functional

$\frac{1}{2}a(v,v) - \Psi(v)$, and since

$$\mathcal{J}(v) = 2\left(\frac{1}{2}a(v,v) - \Psi(v) + \frac{\langle \mathcal{Z}\rangle_M^2 + \lambda_0 V^2}{2}\right),$$

we obtain that σ is also the unique minimum of $\mathcal{J}$. □

In order to compute the unique solution σ of Problem 1, let us write

$$\sigma = \sum_{i=1}^{N+d(m)} \beta_i \omega_i, \tag{8}$$

where

$$\omega_i = \begin{cases} \Phi_\tau(\cdot - x_i) & \text{for } i = 1,\dots,N, \\ q_{i-N} & \text{for } i = N+1,\dots,N+d(m). \end{cases}$$

Then, by substituting (8) in (7) we obtain that $\boldsymbol{\beta} \equiv (\beta_1,\dots,\beta_{N+d(m)})$ is the unique solution of the linear system

$$\boldsymbol{A}X = \boldsymbol{B}, \tag{9}$$

where the element a_{ij} of $\boldsymbol{A}$, for $i,j = 1,\dots,N+d(m)$, is given by

$$a_{ij} = \langle \rho(\omega_i), \rho(\omega_j)\rangle_M + \lambda_0 \int_H \omega_i(x)dx \int_H \omega_j(x)dx + \sum_{k=1}^{m} \lambda_k(\omega_i,\omega_j)_k$$

and

$$\boldsymbol{B} = \left(\langle \rho(w_i), \mathcal{Z}\rangle_M + \lambda_0 V \int_H \omega_i(x)dx\right)_{1\le i\le N+d(m)}.$$

Remark 4. Although the unique solution of Problem 1 depends in fact on m, N, $\mathcal{X}_N$, M, $\mathcal{A}_M$, $\mathcal{Z}$, $\boldsymbol{\lambda}$, V and H, we will denote it just by σ for the sake of simplicity.

4. Convergence result

The aim of this section is to give a convergence result assuring that, under certain technical conditions on the parameters involved in the whole process, the fitting and filling function given by Theorem 2 associated to a given $f \in H^{m+1}(\Omega)$ converges to f in the $\|\cdot\|_m$-norm. In order to establish this convergence theorem we will first recall several results in the existing literature.

Proposition 1 (*Proposition 1 of [22]*)**.** *There exist constants $\varepsilon_0 > 0$ and P and P_1 such that for any $\varepsilon \in (0,\varepsilon_0]$ there exists a finite set $T_\varepsilon \subset \Omega$ satisfying:*

(i) $\overline{B}(t,\varepsilon) \subset \Omega$ *for all* $t \in T_\varepsilon$;
(ii) $\Omega \subset \bigcup_{t\in T_\varepsilon} \overline{B}(t,P\varepsilon)$;
(iii) $\sum_{t\in T_\varepsilon} 1_{\overline{B}(t,P\varepsilon)} \le P_1$;

where $\overline{B}(t,R)$ denotes the closed ball of center t and radius R, and $1_{\overline{B}(t,P\varepsilon)}$ represents the characteristic function of the set $\overline{B}(t,P\varepsilon)$ (i.e., the one taking the value 1 on $\overline{B}(t,P\varepsilon)$ and 0 elsewhere).

Lemma 1. *For any $f \in \mathcal{H}_{\tau,m}$, the variational problem*

$$\underset{\substack{u\in\mathcal{H}_{\tau,m}\\ u|_\Omega = f}}{\text{Minimize}} |u|_{\tau,m}$$

has a unique solution f^Ω that satisfies

$$|f^\Omega|_{\tau,m}^2 = |s_N|_{\tau,m}^2 + |f^\Omega - s_N|_{\tau,m}^2, \tag{10}$$

where s_N is the interpolation spline under tension introduced in Definition 1. Moreover, there exists a constant C (depending on m and Ω) such that

$$|f^\Omega|_{\tau,m} \le C|f|_{\tau,m} \quad \text{for all } f \in \mathcal{H}_{\tau,m}. \tag{11}$$

The proof of this lemma follows a similar pattern to the one of Lemma 2.1 of [20] by taking $\mathcal{H}_{\tau,m}$, $|\cdot|_{\tau,m}$ and s_N instead of $X^m(\mathbb{R}^2)$, $|\cdot|_{m,\tau,\mathbb{R}^2}$ and $f^{\mathcal{A}}$, respectively.

Theorem 3 (*Theorem 2.1 of [20]*). *For any $P \geq 1$ and for any $|\boldsymbol{\alpha}| \leq m$, there exist $R > 0$ (depending on m) and $C > 0$ (depending on P, R, m, $\boldsymbol{\alpha}$ and τ) such that for all $h > 0$ and for all $t \in \mathbb{R}^2$ the ball $B(t, Rh)$ of center t and radius Rh contains $d(m)$ balls $B_1, \ldots, B_{d(m)}$ of radius h such that the inequality*

$$\|D^{\boldsymbol{\alpha}} u\|_{L^2(B(t,PRh))} \leq Ch^{m-|\boldsymbol{\alpha}|} |u|_{m,\tau,B(t,PRh)}$$

holds for all $u \in H^{m+1}(B(t, PRh))$ vanishing at least on one point of each one of the balls $B_1, \ldots, B_{d(m)}$, where $\|\cdot\|_{L^2(X)}$ represents the usual norm $\|u\|_{L^2(X)} = \left(\int_X u(x)^2 dx\right)^{\frac{1}{2}}$ in the space $L^2(X)$.

In what follows we will suppose that the fill-distance defined in (3) satisfies

$$h = o(1), \quad N \to +\infty. \tag{12}$$

Theorem 4. *Let $f \in H^{m+1}(\Omega)$ and s_N be the interpolation spline under tension associated to $\mathcal{X}, \mathcal{F} = \{f(x_i)\}_{i=1}^N$, m and τ introduced in Definition 1. Then, there exist $h_0 > 0$ and $C > 0$ such that for any $h \leq h_0$ it holds:*

$$|f - s_N|_i \leq Ch^{m-i} \|f\|_{m+1}, \ i = 0, \ldots, m.$$

Proof. Let us consider the constants P, P_1 and ε_0 provided by Proposition 1 and the constant R provided by Theorem 3. Let $h_0 = \frac{\varepsilon_0}{R}$ and $h \leq h_0$. Then, if we take $\varepsilon = Rh \leq \varepsilon_0$, there exists a finite set $T_\varepsilon \subset \Omega$ satisfying (i), (ii) and (iii) of Proposition 1. Let, for any $t \in \Omega$, $\{B_i\}_{i=1}^{d(m)}$ be the balls of radius h given by Theorem 3. Then $B_i \subset B(t, Rh) = B(t, \varepsilon) \subset \Omega$. Moreover, by the Definition (3) of h, we have that any ball B of radius h entirely contained in Ω satisfies

$$B \cap \mathcal{X} \neq \varnothing. \tag{13}$$

On the other hand, let $f^\Omega \in \mathcal{H}_{\tau,m}$ be the function given in Lemma 1. It is clear then that $f^\Omega - s_N$ vanishes on $\mathcal{X}$ and therefore, by using (13), we find that the function $(f^\Omega - s_N)|_{B(t,PRh)} = (f - s_N)|_{B(t,PRh)} \in H^{m+1}(B(t, PRh))$ vanishes at least on one point of each one of the balls B_i for $i = 1, \ldots, d(m)$. Therefore, the inequality

$$\|D^{\boldsymbol{\alpha}}(f - s_N)\|_{L^2(B(t,PRh))} \leq Ch^{m-|\boldsymbol{\alpha}|} |f - s_N|_{m,\tau,B(t,PRh)} \tag{14}$$

holds for all $t \in \Omega$ and for all $|\boldsymbol{\alpha}| \leq m$. Moreover, by Proposition 1(ii) and (14) we have that there exists $C > 0$ such that

$$\|D^{\boldsymbol{\alpha}}(f - s_N)\|_{L^2(\Omega)} \leq \left(\sum_{t \in T_\varepsilon} \int_{B(t,PRh)} D^{\boldsymbol{\alpha}}(f - s_N)(x)^2 dx\right)^{\frac{1}{2}} =$$

$$\left(\sum_{t \in T_\varepsilon} \|D^{\boldsymbol{\alpha}}(f - s_N)\|^2_{L^2(B(t,PRh))}\right)^{\frac{1}{2}} \leq$$

$$Ch^{m-|\boldsymbol{\alpha}|} \left(\sum_{t \in T_\varepsilon} |f - s_N|^2_{m,\tau,B(t,PRh)}\right)^{\frac{1}{2}}, \tag{15}$$

and since

$$|f - s_N|^2_{m,\tau,B(t,PRh)} =$$

$$\sum_{|\boldsymbol{\alpha}|=m+1} \frac{(m+1)!}{\boldsymbol{\alpha}!} \int_\Omega 1_{B(t,PRh)} D^{\boldsymbol{\alpha}}(f - s_N)(x)^2 dx +$$

$$\tau^2 \sum_{|\boldsymbol{\alpha}|=m} \frac{m!}{\boldsymbol{\alpha}!} \int_\Omega 1_{B(t,PRh)} D^{\boldsymbol{\alpha}}(f - s_N)(x)^2 dx,$$

by Proposition 1(iii) we obtain

$$\sum_{t \in T_\varepsilon} |f - s_N|^2_{m,\tau,B(t,PRh)} \leq P_1 |f - s_N|^2_{m,\tau,\Omega}.$$

By using this last inequality in (15) we get

$$\|D^{\boldsymbol{\alpha}}(f - s_N)\|_{L^2(\Omega)} \leq Ch^{m-|\boldsymbol{\alpha}|} \sqrt{P_1} |f - s_N|_{m,\tau,\Omega}. \tag{16}$$

Since for all $u \in H^m(\Omega)$ we have

$$|u|_i^2 = \sum_{|\alpha|=i} \|D^\alpha u\|^2_{L^2(\Omega)} \quad \text{for all } i \leq m,$$

from (16) we get that, for all $i \leq m$, there exists $C > 0$ such that

$$|f - s_N|_i \leq Ch^{m-i}|f - s_N|_{m,\tau,\Omega}. \tag{17}$$

Besides, by applying (10) and (11) we get:

$$|f - s_N|_{m,\tau,\Omega} \leq |f^\Omega - s_N|_{m,\tau,\mathbb{R}^2} \leq |f^\Omega|_{m,\tau,\mathbb{R}^2} \leq C\|f\|_{m+1}. \tag{18}$$

Therefore, from (17) and (18) we get that there exists $C > 0$ such that

$$|f - s_N|_i \leq Ch^{m-i}\|f\|_{m+1} \quad \text{for all } i = 0, \ldots, m.$$

Then the result holds. □

Remark 5. The result provided by Theorem 4 is mainly based on the property that the initial basis function Φ_τ is strictly conditionally positive definite. The developed approximation method could have been carried out in any other space of radial basis functions with the same property (for example a radial basis function space generated by Gaussians functions, or thin plate spline functions, or Sobolev splines or Wendland functions).

For any $M \in \mathbb{N}$, let us consider a hole $H_M \subset \Omega$ such that

$$\mu(H_M) = o(1), \quad M \to +\infty, \tag{19}$$

where μ represents the Lebesgue measure, let us suppose that the fill-distance from $\mathcal{A}_M$ to $\Omega - H_M$ satisfies

$$\sup_{x\in\Omega-H_M} \min_{a_i\in\mathcal{A}_M} < x - a_i >_2 = o(1), \quad M \to +\infty, \tag{20}$$

and that $\bigcup_{M\geq 1} H_M \neq \Omega$.

Theorem 5. *Let $f \in H^{m+1}(\Omega)$, with $m \geq 3$, and $\sigma_M^N \in \mathcal{H}$ be the unique solution of Problem 1 for the hole H_M in the space $\mathcal{H}$ defined in (2). Let us suppose that*

$$\lambda_m = o(M), \quad M \to +\infty; \tag{21}$$

$$\lambda_i = o(\lambda_m), \quad M \to +\infty, \quad \textit{for } i = 0, \ldots, m-1; \tag{22}$$

$$\frac{Mh^2}{\lambda_m} = o(1), \quad M \to +\infty. \tag{23}$$

Then

$$\lim_{M\to+\infty} \|\sigma_M^N - f\|_m = 0.$$

Remark 6. The proof of this theorem is divided into four steps: In the first one we obtain some bounds regarding $|\sigma_M^N|_m^2$ and $\langle\rho(\sigma_M^N - f)\rangle_M^2$ as $M \to +\infty$. In the second step we will show that the sequence $\{\sigma_M^N\}$ is bounded in $H^m(\Omega)$. In the third part of the proof we will show that there exists a subsequence of $\{\sigma_M^N\}$ uniformly converging to f over $\overline{\Omega}$. In the last step the thesis of the theorem is proven.

Proof.

(I) From (21) and (23) we obtain that

$$h = o(1), \quad M \to +\infty, \tag{24}$$

and therefore $N \to +\infty$ as $M \to +\infty$. Let $s_N \in \mathcal{H}$ be the restriction to Ω of the interpolation spline under tension associated to $\mathcal{X}^N$, $\mathcal{F} = \{f(x_i)\}_{i=1}^N$, m and τ. Since σ_M^N minimizes the functional $\mathcal{J}$ in $\mathcal{H}$, we have that

$$\langle\rho\left(\sigma_M^N\right) - \rho(f)\rangle_M^2 + \lambda_0\left(\int_{H_M} \sigma_M^N(x)dx - V\right)^2 + \sum_{i=1}^m \lambda_i \left|\sigma_M^N\right|_i^2 \leq$$

$$\langle\rho\left(s_N\right) - \rho(f)\rangle_M^2 + \lambda_0\left(\int_{H_M} s_N(x)dx - V\right)^2 + \sum_{i=1}^m \lambda_i \left|s_N\right|_i^2.$$

Therefore,

$$\left|\sigma_M^N\right|_m^2 \leq \frac{1}{\lambda_m}\langle\rho\left(s_N\right)-\rho(f)\rangle_M^2+\frac{\lambda_0}{\lambda_m}\left(\int_{H_M} s_N(x)dx-V\right)^2+\sum_{i=1}^{m}\frac{\lambda_i}{\lambda_m}\left|s_N\right|_i^2 \tag{25}$$

and

$$\frac{\langle\rho(\sigma_M^N-f)\rangle_M^2}{\lambda_m} \leq \frac{1}{\lambda_m}\langle\rho\left(s_N\right)-\rho(f)\rangle_M^2+\frac{\lambda_0}{\lambda_m}\left(\int_{H_M} s_N(x)dx-V\right)^2+\sum_{i=1}^{m}\frac{\lambda_i}{\lambda_m}\left|s_N\right|_i^2. \tag{26}$$

It is our aim to show that left hand sides of (25) and (26) are bounded and, to this end, we will show that the right hand sides are. By applying Theorem 4 for $i=1,\ldots,m-1$ we obtain that there exists $C>0$ such that

$$\left|s_N\right|_i \leq \left|f-s_N\right|_i+|f|_i \leq Ch^{m-i}+|f|_i \quad \text{for } i=1,\ldots,m-1; \tag{27}$$

and by applying Theorem 4 we obtain that

$$\left|s_N\right|_m \leq \left|f-s_N\right|_m+|f|_m = o(1)+|f|_m, \quad M\to+\infty. \tag{28}$$

On other hand, since $H^{m-1}(\Omega)$ is continuously embedded in $\mathcal{C}^0(\overline{\Omega})$ for $m\geq 3$, there exists $C>0$ such that

$$\|v\|_{\infty,\Omega}=\max_{x\in\overline{\Omega}}|v(x)| \leq C\|v\|_{m-1} \quad \text{for all } v\in H^{m-1}(\Omega). \tag{29}$$

By taking $v=s_N-f$ in (29) and by using Theorem 4 for $i=0,\ldots,m-1$ we get that there exists $K>0$ such that

$$\langle\rho\left(s_N\right)-\rho(f)\rangle_M^2 \leq MC\|s_N-f\|_{m-1}^2 = MC\left(\sum_{i=0}^{m-1}|s_N-f|_i^2\right) \leq$$

$$MKh^2\left(\sum_{i=0}^{m-1}h^{2i}\right). \tag{30}$$

Finally, in a similar way to (29) we get that there exists $C>0$ such that

$$\left(\int_{H_M} s_N(x)dx-V\right)^2 \leq \mu(H_m)^2\left\|s_N-\frac{V}{\mu(H_M)}\right\|_{\infty,\Omega}^2 \leq C\left\|s_N-\frac{V}{\mu(H_M)}\right\|_{m-1}^2,$$

which together with the inequality

$$\left|s_N-\frac{V}{\mu(H_M)}\right|_i \leq |s_N-f|_i+\left|f-\frac{V}{\mu(H_M)}\right|_i \quad \text{for } i=0,\ldots,m-1,$$

and Theorem 4 shows that

$$\left(\int_{H_M} s_N(x)dx-V\right)^2 \text{ is bounded as } M\to+\infty. \tag{31}$$

Now, by using (22), (23), (24), (27), (28), (30) and (31) in (25) and (26) we obtain that

$$\left|\sigma_M^N\right|_m^2 \leq o(1)+|f|_m^2, \quad M\to+\infty, \tag{32}$$

and

$$\frac{\langle\rho(\sigma_M^N-f)\rangle_M^2}{\lambda_m} \leq o(1)+|f|_m^2, \quad M\to+\infty, \tag{33}$$

and, in particular, there exist $C\geq 0$ and $M_0\in\mathbb{N}$ such that for all $M\geq M_0$ it holds

$$\left|\sigma_M^N\right|_m^2 \leq C \tag{34}$$

and

$$\langle\rho(\sigma_M^N-f)\rangle_M^2 \leq \lambda_m C. \tag{35}$$

(II) By (20) we know that there exists $r_0>0$ such that for all $r<r_0$ there exists a natural M_r such that for all $M\geq M_r$ and for all $x\in\Omega-\bigcup_{M\geq 1}H_M$

$$\text{there exists } a\in\mathcal{A}_M \text{ such that } a\in B(x,r). \tag{36}$$

Let $\mathcal{A}^0=\{a_1^0,\ldots,a_{d(m)}^0\}$ be a $\Pi_{m-1}(\mathbb{R}^2)$-unisolvent subset of $\Omega-\bigcup_{M\geq 1}H_M$ and let $r_0'\leq r_0$ such that $\overline{B}\left(a_j^0,r_0'\right)\subset\Omega-\bigcup_{M\geq 1}H_M$ for all $j=1,\ldots,d(m)$. Then, if $0<r<r_0'$ and $x\in\overline{B}(a_j^0,r_0'-r)$ by (36) we can find, for all $M\geq M_r$, a

point $a \in \mathcal{A}_M$ such that $\langle a - x\rangle_2 \leq r$ and therefore,

$$\langle a - a_j^0\rangle_2 \leq \langle a - x\rangle_2 + \langle x - a_j^0\rangle_2 \leq r + r_0' - r = r_0'.$$

Thus we conclude that

$$\overline{B}(a_j^0, r_0' - r) \subset \bigcup_{a \in \mathcal{A}_M \cap \overline{B}\left(a_j^0, r_0'\right)} \overline{B}\,(a, r) \tag{37}$$

for all $0 < r < r_0'; j = 1, \ldots, d(m)$ and $M \geq M_r$.

Letting $N_j = card\left(\mathcal{A}_M \cap \overline{B}\left(a_j^0, r_0'\right)\right)$, from (37) we obtain

$$(r_0' - r)^2 \leq N_j r^2 \quad \text{for all } 0 < r < r_0' \text{ and } j = 1, \ldots, d(m). \tag{38}$$

Now, let M_0 be the lowest integer such that $\frac{1}{M_0} < r_0'$. Then, from (38) we deduce that for all $M \geq M_0$ we have

$$\left(r_0' - \frac{1}{M_0}\right)^2 \leq N_j \left(\frac{1}{M}\right)^2 \Longrightarrow N_j \geq M^2 \left(r_0' - \frac{1}{M_0}\right)^2. \tag{39}$$

On other hand, by applying (35) we obtain

$$\sum_{\mathcal{A}_M \cap \overline{B}\left(a_j^0, r_0'\right)} \left|\sigma_M^N(a) - f(a)\right|^2 \leq \langle \rho(\sigma_M^N - f)\rangle^2 \leq \lambda_m C$$

and therefore, by (21), we get that

$$\sum_{\mathcal{A}_M \cap \overline{B}\left(a_j^0, r_0'\right)} \left|\sigma_M^N(a) - f(a)\right|^2 = o(M), \quad M \to +\infty. \tag{40}$$

Since $\mathcal{A}_M \cap \overline{B}\left(a_j^0, r_0'\right)$ is a finite set, we can find, for $j = 1, \ldots, d(m)$,

$$a_j^M \in \mathcal{A}_M \cap \overline{B}\left(a_j^0, r_0'\right) \tag{41}$$

such that

$$\left|\sigma_M^N(a_j^M) - f(a_j^M)\right| = \min_{a \in \mathcal{A}_M \cap \overline{B}\left(a_j^0, r_0'\right)} \left|\sigma_M^N(a) - f(a)\right|$$

and, as a consequence, by using (39) we get

$$\left|\sigma_M^N(a_j^M) - f(a_j^M)\right|^2 \leq \frac{\sum_{\mathcal{A}_M \cap \overline{B}\left(a_j^0, r_0'\right)} \left|\sigma_M^N(a) - f(a)\right|^2}{N_j} \leq$$

$$\frac{\sum_{\mathcal{A}_M \cap \overline{B}\left(a_j^0, r_0'\right)} \left|\sigma_M^N(a) - f(a)\right|^2}{M^2 \left(r_0' - \frac{1}{M_0}\right)^2}.$$

By using (40) we derive

$$\left|\sigma_M^N(a_j^M) - f(a_j^M)\right| = o(1), \quad M \to +\infty, \quad \text{for all } j = 1, \ldots, d(m),$$

from where we conclude

$$\left|\sigma_M^N(a_j^M)\right| \leq \left|\sigma_M^N(a_j^M) - f(a_j^M)\right| + \left|f(a_j^M)\right| \text{ is bounded for all } j = 1, \ldots, d(m). \tag{42}$$

Let us now consider the set $\mathcal{B}^M$ consisting of all points $\{a_1^M, \ldots, a_{d(m)}^M\}$ defined in (41). Then, by using (34), (42) and Proposition V-1.2 of [23] for $B = \mathcal{B}^M$, we get that there exist M_1 and $C > 0$ such that $\|\sigma_M^N\| \leq C$ for all $M \geq M_1$ and therefore, the sequence

$$\left\{\sigma_M^N\right\}_{M \geq M_1} \text{ is bounded in } H^m(\Omega). \tag{43}$$

(III) As a consequence of (43), there exists a subsequence $\{\sigma_{M_\ell}^{N_\ell}\}_{\ell \in \mathbb{N}}$ of $\{\sigma_M^N\}_{M \geq M_1}$, with $N_\ell = N(M_\ell)$, such that

$$\{\sigma_{M_\ell}^{N_\ell}\}_{\ell \in \mathbb{N}} \text{ converges weakly to an element } f^* \in H^m(\Omega) \tag{44}$$

and, since $H^m(\Omega)$ is compactly embedded in $C^0(\overline{\Omega})$, we deduce from (44) that

$$\{\sigma_{M_\ell}^{N_\ell}\}_{\ell \in \mathbb{N}} \text{ converges uniformly over } \overline{\Omega} \text{ to } f^*. \tag{45}$$

Let us suppose that $f^* \neq f$. Then, by using (19), there would exist $\ell_0 \in \mathbb{N}$, a nonempty open subset $\Omega_0 \subset \Omega$ such that $\Omega_0 \cap (\Omega - \cup_{\ell \geq \ell_0} H^{M_\ell}) \neq \varnothing$ and a real number τ such that $|f(x) - f^*(x)| > \tau$ for all $x \in \Omega_0$, but from (45) we get that there exists $\ell_1 \in \mathbb{N}$ such that

$$|f^*(x) - \sigma_{M_\ell}^{N_\ell}(x)| \leq \frac{\tau}{2} \text{ for all } \ell \geq \ell_1 \text{ and } x \in \Omega_0.$$

As a consequence, for all $\ell \geq \ell_1$ and $x \in \Omega_0$ we would have

$$|f(x) - \sigma_{M_\ell}^{N_\ell}(x)| \geq |f(x) - f^*(x)| - |f^*(x) - \sigma_{M_\ell}^{N_\ell}(x)| > \frac{\tau}{2}. \tag{46}$$

Let now $\ell_2 \in \mathbb{N}$ be such that $M_{\ell_2} \geq \max\{M_{\ell_0}, M_{\ell_1}\}$. Then, if we take $z \in \Omega_0 \cap (\Omega - \cup_{\ell \geq \ell_0} H^{M_\ell})$ and $r_0' \leq r_0$ (defined before Eq. (36)) such that $\overline{B}(z, r_0') \subset \Omega_0 \cap (\Omega - \cup_{\ell \geq \ell_0} H^{M_\ell})$, a similar argument to the one developed in Part (II) of this proof for the points $\{a_i^0\}_{i=1}^{d(m)}$ will lead to a sequence $\{a^{M_\ell}\}_{\ell \geq \ell_2}$, with $a^{M_\ell} \in \mathcal{A}_{M_\ell} \cap \overline{B}\left(z, r_0'\right) \subset \Omega_0$ for all $\ell \geq \ell_2$ such that

$$\left| f(a^{M_\ell}) - \sigma_{M_\ell}^{N_\ell}(a^{M_\ell}) \right| = o(1), \quad M_\ell \to +\infty,$$

which contradicts (46). Therefore, $f^* = f$.

(IV) By using (32) and (44) in the expression

$$\left| \sigma_{M_\ell}^{N_\ell} - f \right|_m^2 = \left| \sigma_{M_\ell}^{N_\ell} \right|_m^2 + |f|_m^2 - 2\left(\sigma_{M_\ell}^{N_\ell}, f\right)_m$$

it follows that

$$\lim_{\ell \to \infty} \left| \sigma_{M_\ell}^{N_\ell} - f \right|_m^2 = 0. \tag{47}$$

Moreover, since $H^m(\Omega)$ is compactly embedded in $H^{m-1}(\Omega)$, again from (44) we deduce that

$$\lim_{\ell \to \infty} \sigma_{M_\ell}^{N_\ell} = f \quad \text{in } H^{m-1}(\Omega)$$

and therefore

$$\lim_{\ell \to \infty} \left\| \sigma_{M_\ell}^{N_\ell} - f \right\|_{m-1} = 0,$$

which jointly with (47) allows us to assure that

$$\lim_{\ell \to \infty} \left\| \sigma_{M_\ell}^{N_\ell} - f \right\|_m = 0. \tag{48}$$

Finally, let us suppose that the thesis of theorem is not satisfied. Then, there would exist a subsequence $\{\sigma_{M_\ell'}^{N_\ell'}\}_{\ell \in \mathbb{N}}$ of $\{\sigma_M^N\}_{M \in \mathbb{N}}$, with $N_\ell' = N(M_\ell')$, and a real number $\tau > 0$ such that

$$\left\| \sigma_{M_\ell'}^{N_\ell'} - f \right\|_m > \tau \quad \text{for all } \ell \in \mathbb{N}. \tag{49}$$

But from (43) we have that the sequence $\{\sigma_{M_\ell'}^{N_\ell'}\}_{\ell \in \mathbb{N}}$ is bounded in $H^m(\Omega)$ and thus, by applying the same argument developed between (43)–(48) we could find a subsequence $\{\sigma_{M_\ell''}^{N_\ell''}\}_{\ell \in \mathbb{N}}$ of $\{\sigma_{M_\ell'}^{N_\ell'}\}_{\ell \in \mathbb{N}}$, with $N_\ell'' = N(M_\ell'')$, such that

$$\lim_{\ell \to \infty} \left\| \sigma_{M_\ell''}^{N_\ell''} - f \right\|_m = 0,$$

which contradicts (49). □

5. Numerical and graphical examples

In order to show the performance of the method proposed, in this section we present several graphical and numerical examples. The ones associated to Experiments 1 to 5 have been carried out under the following common frame:

- The domain $\Omega = (0, 1) \times (0, 1)$.
- $m = 2$; the basis $\{1, x, y, x^2, xy, y^2\}$ of $\Pi_2(\mathbb{R}^2)$ and a set $\mathcal{X}$ consisting of $N = 25$ uniformly distributed centers, in such a way that the finite-dimensional subspace of $H^3(\mathbb{R}^2)$ is the one generated by

  $$\{\Phi_\tau(\cdot - x_1), \ldots, \Phi_\tau(\cdot - x_{25}), 1, x, y, x^2, xy, y^2\}.$$

  Observe that these values of N and m lead, in all examples, to linear systems (9) of dimension 31.
- A dataset of fitting points $\mathcal{A} = \{a_1, \ldots, a_{1500}\}$ consisting of $M = 1500$ points randomly distributed in $\Omega - H$ and the set of real fitting data $\mathcal{Z} = \{f(a_i)\}_{i=1}^{1500}$, where f is the test function considered in each one of the examples.

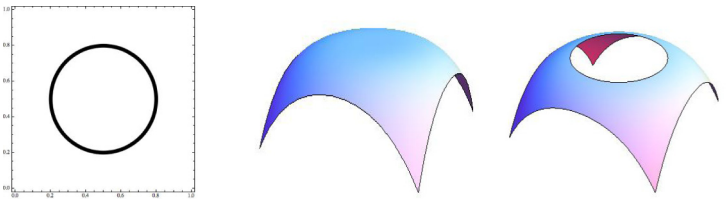

Fig. 1. Hole H_1 and plots of f_1 over Ω and over $\Omega - H_1$.

- The value $\tau = 1$. Regarding this choice, it is worthy to mention that we have tested the values $\tau = 10^i$ for $i = -2, -1, 0, 1, 2$, but the best results are obtained for $i = 0$ (see Table 3).
- Estimations E_{out} and E_{in} of the RMSE relative errors of the fitting and of the filling patches σ over $\Omega - H$ and over H, respectively, given by

$$E_{out} = \left(\frac{\sum_{i=1}^{2000} (f(c_i) - \sigma(c_i))^2}{\sum_{i=1}^{2000} f(c_i)^2} \right)^{1/2}; E_{in} = \left(\frac{\sum_{i=1}^{2000} (f(d_i) - \sigma(d_i))^2}{\sum_{i=1}^{2000} f(d_i)^2} \right)^{1/2},$$

where $\{c_i\}_{i=1}^{2000}$ are random points in $\Omega - H$ and $\{d_i\}_{i=1}^{2000}$ are random points in H.

For the numerical results shown in Tables 1 to 3 some of the previous parameters have been changed in order to highlight their impact in the final results.

Next we show five different experiments. In all of them we provide: the hole H_i and its plot, the test function f_i and its plot with and without hole, the value of the parameters $\boldsymbol{\lambda} = \{\lambda_0, \lambda_1, \lambda_2\}$ considered and numerical and graphical examples for three different values of the volume constraint V: V^e, which has been considered to be the exact signed-volume $V^e = \int_{H_i} f_i$ of the function f_i over H_i (except for the test function f_4, in which we have replaced the exact value $V^e = 0$ for a very close value for numerical purposes), and V^+ and V^-, which have been considered to be values slightly upper and lower to V^e, respectively. In all cases we give the plot of the fitting–filling σ (the point of view of the figures is chosen in order to properly show the effect of imposing the signed-volume constraint), the values of the volume constraints $\{V^e, V^+, V^-\}$; the value of $\int_{H_i} \sigma$ and the relative error E_{out}. In the case $V = V^e$ we also give the value of E_{in} (this relative error has no sense at all in the cases $V = V^+, V^-$). In all the experiments, the fitting–filling σ better satisfy the volume constraint in the case $V = V^e$. To check it, we just have to consider a measure of the relative error $\frac{\left(V - \int_H \sigma\right)^2}{V^2}$. Moreover, regarding the cases $V = V^+, V^-$, we can observe that the lower the value $\frac{(V - V^e)^2}{V^2}$ is, the better the fitting–filling σ will satisfy the volume constraint. In other words, the farther the imposed signed-volume V of σ over H_i is from the exact one V^e, the worst such a volume constraint will be satisfied.

5.1. Experiment 1: Cosine function f_1

▷ $f_1(x, y) = \cos\left((x - 0.5)^2 + (y - 0.5)^2\right) - \cos(0.09)$.
▷ $H_1 \equiv \frac{(x-0.5)^2}{0.3^2} + \frac{(y-0.5)^2}{0.3^2} = 1$.
▷ $\boldsymbol{\lambda} = \{10^3, 10^{-9}, 10^{-10}\}$ (see Figs. 1 and 2).

5.2. Experiment 2: Franke's function f_2

▷ $f_2(x, y) = 0.75e^{-\frac{(9y-2)^2+(9x-2)^2}{4}} + 0.75e^{-\frac{(9y+1)^2}{49} - \frac{(9x+1)}{10}} + 0.5e^{-\frac{(9y-7)^2+(9x-3)^2}{4}} - 0.2e^{-(9y-4)^2+(9x-7)^2}$. ▷ $H_2 \equiv 0.5(x - 0.4)^2 + 0.7(y - 0.6)^2 = 0.25^2$.
▷ $\boldsymbol{\lambda} = \{10^3, 10^{-7}, 10^{-8}\}$ (see Figs. 3 and 4).

5.3. Experiment 3: Semisphere function f_3

▷ $f_3(x, y) = \begin{cases} \sqrt{0.5^2 - (x - 0.5)^2 - (y - 0.5)^2} & \text{if } (x - 0.5)^2 - (y - 0.5)^2 \leq 0.5^2, \\ 0 & \text{otherwise.} \end{cases}$
▷ $H_3 \equiv \frac{(x-0.5)^2}{0.3^2} + \frac{(y-0.5)^2}{0.3^2} = 1$.
▷ $\boldsymbol{\lambda} = \{10^3, 10^{-9}, 10^{-9}\}$ (see Figs. 5 and 6).

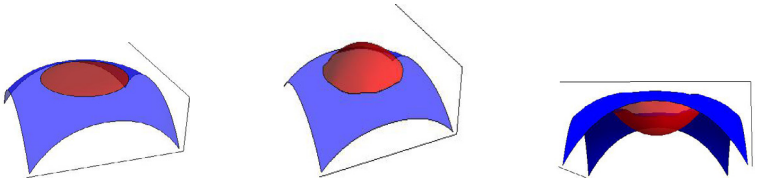

$V^e = 7.62 \cdot 10^{-4}$
$\int_{H_1} \sigma = 7.15 \cdot 10^{-4}$
$E_{out} = 5.39 \cdot 10^{-4}$
$E_{in} = 1.19 \cdot 10^{-3}$

$V^+ = 10^{-2}$
$\int_{H_1} \sigma = 8.54 \cdot 10^{-3}$
$E_{out} = 6.83 \cdot 10^{-4}$

$V^- = -10^{-2}$
$\int_{H_1} \sigma = -8.41 \cdot 10^{-3}$
$E_{out} = 8.6 \cdot 10^{-4}$

Fig. 2. Numerical and graphical results for f_1.

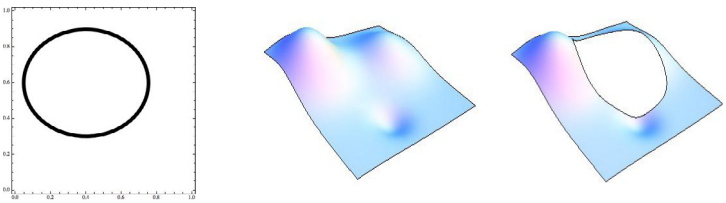

Fig. 3. Hole H_2 and plots of f_2 over Ω and over $\Omega - H_2$.

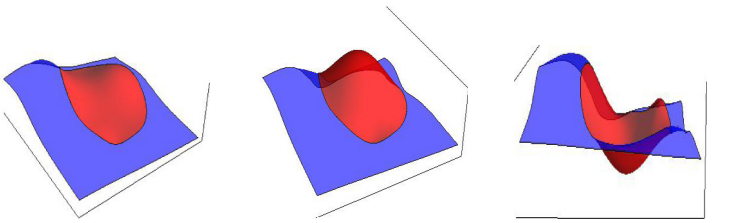

$V^e = 0.1434$
$\int_{H_2} \sigma = 01411$
$E_{out} = 1.92 \cdot 10^{-3}$
$E_{in} = 7.34 \cdot 10^{-3}$

$V^+ = 0.3$
$\int_{H_2} \sigma = 0.292$
$E_{out} = 4.04 \cdot 10^{-3}$

$V^- = 10^{-3}$
$\int_{H_2} \sigma = 0.013$
$E_{out} = 6.54 \cdot 10^{-3}$

Fig. 4. Numerical and graphical results for f_2.

Fig. 5. Hole H_3 and plots of f_3 over Ω and over $\Omega - H_3$.

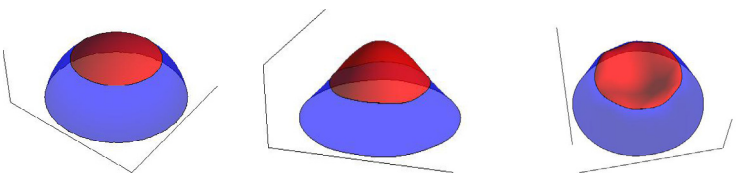

$V^e = 0.1277$
$\int_{H_3} \sigma = 0.1271$
$E_{out} = 5.32 \cdot 10^{-3}$
$E_{in} = 6.13 \cdot 10^{-3}$

$V^+ = 0.23$
$\int_{H_3} \sigma = 0.2196$
$E_{out} = 7.87 \cdot 10^{-3}$

$V^- = 0.07$
$\int_{H_3} \sigma = 0.07891$
$E_{out} = 9.17 \cdot 10^{-3}$

Fig. 6. Numerical and graphical results for f_3.

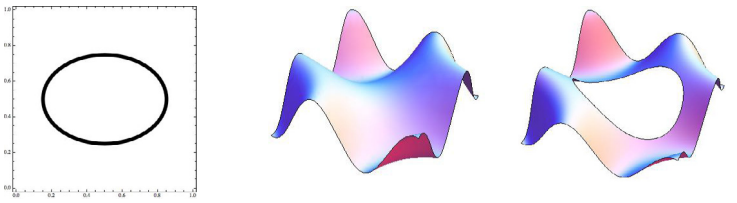

Fig. 7. Hole H_4 and plots of f_4 over Ω and over $\Omega - H_4$.

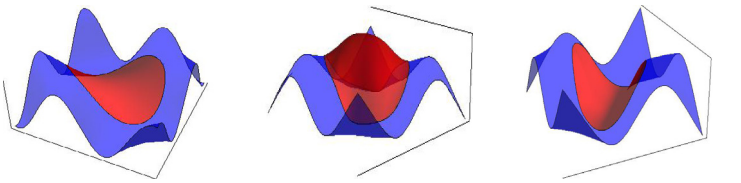

$V^e = 10^{-6}$
$\int_{H_4} \sigma = 3.17 \cdot 10^{-3}$
$E_{out} = 5.06 \cdot 10^{-5}$
$E_{in} = 9.43 \cdot 10^{-5}$

$V^+ = 0.1$
$\int_{H_4} \sigma = 0.0992$
$E_{out} = 2.78 \cdot 10^{-4}$

$V^- = -0.1$
$\int_{H_4} \sigma = -0.0987$
$E_{out} = 8.65 \cdot 10^{-4}$

Fig. 8. Numerical and graphical results for f_4.

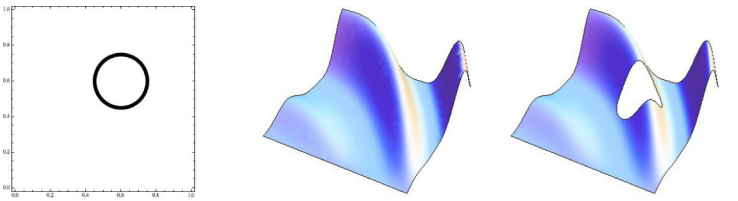

Fig. 9. Hole H_5 and plots of f_5 over Ω and over $\Omega - H_5$.

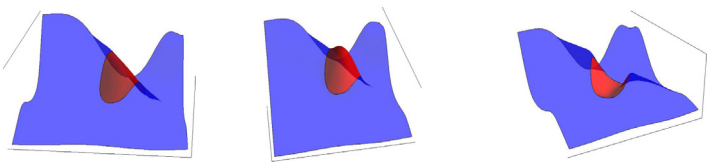

$V^e = 1.45 \cdot 10^{-2}$
$\int_{H_5} \sigma = 1.48 \cdot 10^{-2}$
$E_{out} = 8.21 \cdot 10^{-4}$
$E_{in} = 7.19 \cdot 10^{-3}$

$V^+ = 2.5 \cdot 10^{-2}$
$\int_{H_5} \sigma = 2.34 \cdot 10^{-2}$
$E_{out} = 1.87 \cdot 10^{-3}$

$V^- = 10^{-2}$
$\int_{H_5} \sigma = 1.75 \cdot 10^{-2}$
$E_{out} = 1.32 \cdot 10^{-3}$

Fig. 10. Numerical and graphical results for f_5.

5.4. Experiment 4: Sinusoidal function f_4

- $f_4(x, y) = \sin\left(2\pi^2(x - 0.5)(y - 0.5)\right)$.
- $H_4 \equiv \frac{(x-0.5)^2}{0.35^2} + \frac{(y-0.5)^2}{0.25^2} = 1$.
- $\boldsymbol{\lambda} = \{10^2, 10^{-7}, 10^{-7}\}$ (see Figs. 7 and 8).

5.5. Experiment 5: Nielson's function f_5

- $f_5(x, y) = \frac{y}{2}\cos^4\left(4(x^2 + y - 1)\right)$.
- $H_5 \equiv \frac{(x-0.6)^2}{0.15^2} + \frac{(y-0.6)^2}{0.15^2} = 1$.
- $\boldsymbol{\lambda} = \{10^3, 10^{-9}, 10^{-10}\}$ (see Figs. 9 and 10).

Table 1
Error estimations for f_1 with $M = 5000$, $N = 25$ and $R = 0.3$.

V	λ_0	λ_1	λ_2	E_{out}	E_V
V^e	0	10^{-11}	10^{-11}	$1.5697 \cdot 10^{-4}$	$1.2239 \cdot 10^{-3}$
V^e	10^3	10^{-11}	10^{-11}	$2.4315 \cdot 10^{-4}$	$6.2725 \cdot 10^{-5}$
$1 \cdot 10^{-2}$	10^3	10^{-11}	10^{-11}	$1.1757 \cdot 10^{-3}$	$3.6638 \cdot 10^{-4}$
$-5 \cdot 10^{-3}$	10^3	10^{-11}	10^{-11}	$1.0406 \cdot 10^{-3}$	$3.3040 \cdot 10^{-4}$
V^e	10^3	10^3	10^3	$1.9989 \cdot 10^{-2}$	$7.0278 \cdot 10^{-3}$
V^e	10^3	10^3	10^{-3}	$1.8353 \cdot 10^{-2}$	$6.5112 \cdot 10^{-3}$
V^e	10^3	10^3	10^{-11}	$1.8353 \cdot 10^{-2}$	$6.5112 \cdot 10^{-3}$
V^e	10^3	10^{-3}	10^3	$1.9971 \cdot 10^{-2}$	$7.0199 \cdot 10^{-3}$
V^e	10^3	10^{-3}	10^{-3}	$2.4036 \cdot 10^{-4}$	$1.4467 \cdot 10^{-4}$
V^e	10^3	10^{-3}	10^{-11}	$2.3462 \cdot 10^{-4}$	$1.4233 \cdot 10^{-4}$
V^e	10^3	10^{-11}	10^3	$1.9970 \cdot 10^{-2}$	$7.0199 \cdot 10^{-3}$
V^e	10^3	10^{-11}	10^{-3}	$2.4022 \cdot 10^{-4}$	$1.4496 \cdot 10^{-4}$
V^e	10^3	10^{-11}	10^{-11}	$2.3464 \cdot 10^{-4}$	$1.4576 \cdot 10^{-4}$
V^e	10^{-3}	10^{-11}	10^{-11}	$1.5179 \cdot 10^{-4}$	$1.2565 \cdot 10^{-3}$
V^e	1	10^{-11}	10^{-11}	$1.5176 \cdot 10^{-4}$	$1.2472 \cdot 10^{-3}$
V^e	10^3	10^{-11}	10^{-11}	$2.3464 \cdot 10^{-4}$	$1.4576 \cdot 10^{-4}$
V^e	10^6	10^{-11}	10^{-11}	$2.5229 \cdot 10^{-4}$	$7.2390 \cdot 10^{-7}$
V^e	10^9	10^{-11}	10^{-11}	$2.5234 \cdot 10^{-4}$	$8.9753 \cdot 10^{-6}$

Table 2
Error estimations for f_1 with $\lambda_0 = 10^3$ and $\lambda_1 = \lambda_2 = 10^{-11}$.

M	N	R	$V = \int_H f_1(x)dx$	E_{out}	E_V
500	25	0.3	$7.6279 \cdot 10^{-4}$	$2.9856 \cdot 10^{-4}$	$2.9601 \cdot 10^{-5}$
1500	25	0.3	$7.6279 \cdot 10^{-4}$	$2.5657 \cdot 10^{-4}$	$5.6449 \cdot 10^{-5}$
2500	25	0.3	$7.6279 \cdot 10^{-4}$	$2.4738 \cdot 10^{-4}$	$8.7719 \cdot 10^{-5}$
5000	25	0.3	$7.6279 \cdot 10^{-4}$	$2.3464 \cdot 10^{-4}$	$1.4576 \cdot 10^{-4}$
10000	25	0.3	$7.6279 \cdot 10^{-4}$	$2.2211 \cdot 10^{-4}$	$2.5092 \cdot 10^{-4}$
5000	16	0.3	$7.6279 \cdot 10^{-4}$	$4.9390 \cdot 10^{-4}$	$6.1590 \cdot 10^{-4}$
5000	25	0.3	$7.6279 \cdot 10^{-4}$	$2.3464 \cdot 10^{-4}$	$1.4576 \cdot 10^{-4}$
5000	36	0.3	$7.6279 \cdot 10^{-4}$	$1.6842 \cdot 10^{-4}$	$9.5893 \cdot 10^{-5}$
5000	49	0.3	$7.6279 \cdot 10^{-4}$	$9.1406 \cdot 10^{-5}$	$2.2702 \cdot 10^{-5}$
5000	25	0.4	$-1.0754 \cdot 10^{-4}$	$4.6544 \cdot 10^{-4}$	$6.1590 \cdot 10^{-4}$
5000	25	0.3	$7.6279 \cdot 10^{-4}$	$2.3464 \cdot 10^{-4}$	$1.4576 \cdot 10^{-4}$
5000	25	0.2	$4.7509 \cdot 10^{-4}$	$2.2362 \cdot 10^{-4}$	$9.7961 \cdot 10^{-5}$
5000	25	0.1	$1.2663 \cdot 10^{-4}$	$2.7119 \cdot 10^{-4}$	$5.5636 \cdot 10^{-5}$
5000	25	0.05	$3.1779 \cdot 10^{-5}$	$2.8677 \cdot 10^{-4}$	$2.9529 \cdot 10^{-6}$

To conclude the experimental section, we also provide several tables of errors obtained for different experiments carried out with the test function f_1. In these tables we also include an estimation

$$E_V = \left| V - \frac{\mu(H)}{2000} \sum_{i=1}^{2000} \sigma(\xi_i) \right|$$

of the absolute error in the signed volume over the hole H, where $\{\xi_1, \ldots, \xi_{2000}\}$ is a set of random points in H; $\mu(H)$ is the Lebesgue measure of the hole H; N is the number of the uniformly distributed centers $\mathcal{X}$; M is the number of the randomly fitting points $\mathcal{A} \subset \Omega - H$ and σ is the corresponding fitting-filling function. Experiments have been carried out over the hole H defined as the circle of radius R centered at $(x, y) = (0.5, 0.5)$. In what follows, V^e denotes the exact volume $\int_H f_1(x)dx = 7.6279 \cdot 10^{-4}$ for $R = 0.3$.

In Table 1 we can observe that the experiments with higher values of λ_0 lead to better results of E_V, while higher values of λ_1 and λ_2 lead to worse results of E_{out}. This is reasonable insofar as λ_0 weights the fulfilling of the volume constraint in the functional (6), while λ_1 and λ_2 weight the smoothness of the function. In Table 2 we present three different experiments: first, we consider an increasing number of data points M for the fixed hole $R = 0.3$ and for a fixed set of centers ($N = 25$). Secondly, we consider an increasing number of centers N for the same fixed hole $R = 0.3$ and for a fixed set of data points ($M = 5000$). These two experiments show that the higher M and N, the lower the values of E_{out} are, as it is expected from the convergence Theorem 5. The last one experiment in Table 2 rely on the hole: we fix the set of centers and the set of data points, and we consider a set of decreasing holes. In this case, we check that the smaller the hole H is, the lower the values of E_V are, as expected. In Table 3 we can observe that the best results are obtained for the value $\tau = 1$ of the tension parameter.

Table 3
Error estimations for f_1 for different values of τ, N and M with $\lambda_0 = 10^3$, $\lambda_1 = \lambda_2 = 10^{-11}$, $R = 0.3$ and $V = V^e$.

τ	N	M	E_{out}	E_V
0.01	49	500	$5.4992 \cdot 10^{-3}$	$2.6721 \cdot 10^{-3}$
		5000	$4.2032 \cdot 10^{-3}$	$4.3198 \cdot 10^{-3}$
		10000	$4.3596 \cdot 10^{-3}$	$4.2582 \cdot 10^{-3}$
0.1	49	500	$4.23562 \cdot 10^{-4}$	$3.3476 \cdot 10^{-5}$
		5000	$5.8219 \cdot 10^{-4}$	$2.0711 \cdot 10^{-4}$
		10000	$5.4637 \cdot 10^{-4}$	$2.2105 \cdot 10^{-4}$
1	49	500	$1.2667 \cdot 10^{-4}$	$1.1275 \cdot 10^{-6}$
		5000	$9.4148 \cdot 10^{-5}$	$8.1315 \cdot 10^{-6}$
		10000	$1.2860 \cdot 10^{-4}$	$1.5188 \cdot 10^{-5}$
10	49	500	$7.6448 \cdot 10^{-4}$	$1.6968 \cdot 10^{-6}$
		5000	$2.2409 \cdot 10^{-4}$	$2.2457 \cdot 10^{-5}$
		10000	$2.0132 \cdot 10^{-4}$	$1.0202 \cdot 10^{-5}$
100	49	500	$6.2868 \cdot 10^{-4}$	$2.7189 \cdot 10^{-6}$
		5000	$3.6728 \cdot 10^{-4}$	$2.3190 \cdot 10^{-5}$
		10000	$3.5515 \cdot 10^{-4}$	$6.5796 \cdot 10^{-5}$

Table 4
Orders of the relative errors E_{in} when filling with different methods.

	Sinusoidal	Semisphere	Franke	Nielson
This work	$\mathbf{10^{-5}}$	$\mathbf{10^{-3}}$	$\mathbf{10^{-3}}$	$\mathbf{10^{-3}}$
Cartesian wireframe in [24]	10^{-5}	10^{-2}	10^{-3}	10^{-3}
Shape-preserving criteria in [8]	–	10^{-4}	10^{-4}	10^{-3}
Minimal criteria in [8]	–	10^{-3}	10^{-3}	10^{-1}

6. Conclusions

We have developed a method that constructs functions from surface points outside a given hole. The method produces a smooth function where some parameters are manageable, including a volume objective. Radial basis functions are used, so the number of functions needed to build the resulting function is smaller and the computational cost is reduced compared to other spline based methods. Indeed, we can observe that relative errors of similar order to those obtained by means of finite elements in other related papers are obtained in this work with much lower computational costs: To state this affirmation we just have to observe that the order of the relative errors obtained in the numerical part of this work, associated to a linear system of dimension 31, are similar to the ones obtained in other papers (see e.g. [24]) by solving much larger linear systems. More precisely, in [24] the triangulation considered consists of 256 knots, which leads to linear systems of order 768. It is also worthy to mention that this reduction in the dimension of the linear systems translates into a reduction of the computing time. More precisely, the examples carried out in this work take over 20% of time needed to carry out the examples in [24]. The next table presents a comparative of the orders of the relative errors E_{in} obtained with different methods (see Table 4):

Data availability

No data was used for the research described in the article.

Acknowledgments

This work was supported by FEDER/Junta de Andalucía-Consejería de Transformación Económica, Industria, Conocimiento y Universidades (Research Project A-FQM-76-UGR20, University of Granada) and by the Junta de Andalucía (Research Groups FQM-191 and TEP-190). Funding for open access charge: Universidad de Granada / CBUA.

References

[1] C. Wang, P. Hu, A hole-filling algorithm for triangular meshes in engineering, Int. J. Comput. Methods Eng. Sci. Mech. 14 (5) (2013) 465–571, http://dx.doi.org/10.1080/15502287.2013.784385.
[2] X. Li, X. Li, Filling the holes of 3D body scan line point cloud, in: 2nd International Conference on Advanced Computer Control, 2010, pp. 334–338, http://dx.doi.org/10.1109/ICACC.2010.5486910.
[3] L.-C. Wang, Y.-C. Hung, Hole filling of triangular mesh segments using systematic grey prediction, Comput. Aided Des. 44 (12) (2012) 1182–1189, http://dx.doi.org/10.1016/j.cad.2012.07.007.
[4] Z. Yang, Y. Sun, J. Cui, Z. Yang, The hole-filling method and multiscale algorithm for the heat transfer performance of periodic porous materials, J. Comput. Appl. Math. 311 (2017) 583–598, http://dx.doi.org/10.1016/j.cam.2016.08.017.

[5] J. Branch, F. Prieto, P. Boulanger, Automatic hole-filling of triangular meshes using local radial basis functions, in: 3rd International Symposium on 3D Data Processing, Visualization and Transmission, 2006, http://dx.doi.org/10.1109/3DPVT.2006.33.
[6] D. Barrera, M.A. Fortes, P. González, M. Pasadas, Filling polygonal holes with minimal energy surfaces on Powell–Sabin type triangulations, J. Comput. Appl. Math. 234 (4) (2010) 1058–1068, http://dx.doi.org/10.1016/j.cam.2009.04.012.
[7] M.A. Fortes, P. González, M. Pasadas, M.L. Rodríguez, A hole filling method for surfaces by using C^1-Powell–Sabin splines. Estimation of the smoothing parameters, Math. Comput. Simul. 81 (10) (2011) 2150–2161, http://dx.doi.org/10.1016/j.matcom.2010.12.003.
[8] M.A. Fortes, P. González, A. Palomares, M. Pasadas, Filling holes with shape preserving conditions, Math. Comput. Simulation 118 (2015) 198–212, http://dx.doi.org/10.1016/j.matcom.2014.12.008.
[9] M.A. Fortes, P. González, A. Palomares, M. Pasadas, Filling holes with geometric and volumetric constraints, Comput. Math. Appl. 74 (4) (2017) 671–683, http://dx.doi.org/10.1016/j.camwa.2017.05.009.
[10] T. Ju, Fixing geometric errors on polygonal models: A survey, J. Comput. Sci. Tech. 24 (1) (2009) 19–29, http://dx.doi.org/10.1007/s11390-009-9206-7.
[11] M.A. Fortes, E. Medina, Fitting missing data by means of adaptive meshes of Bézier curves, Math. Comput. Simulation 191 (2022) 33–48, http://dx.doi.org/10.1016/j.matcom.2021.07.025.
[12] G. Jakleč, T. Kanduč, Hermite interpolation by triangular cubic patches with small Willmore energy, Int. J. Comput. Math. 90 (9) (2013) 1881–1898, http://dx.doi.org/10.1080/00207160.2013.765559.
[13] M.A. Fortes, P. González, M. Pasadas, M.L. Rodríguez, Hole filling on surfaces by discrete variational splines, Appl. Numer. Math. 62 (9) (2012) 1050–1060, http://dx.doi.org/10.1016/j.apnum.2011.11.003.
[14] D. Barrera, M.A. Fortes, P. González, M. Pasadas, Minimal energy C^r-surfaces on uniform Powell–Sabin type meshes: Estimation of the smoothing parameters, Math. Comput. Simulation 77 (2–3) (2008) 161–169, http://dx.doi.org/10.1016/j.matcom.2007.08.020.
[15] A. Kouibia, M. Pasadas, Approximation by discrete variational splines, J. Comput. Appl. Math. 116 (1) (2000) 145–156, http://dx.doi.org/10.1016/S0377-0427(99)00316-7.
[16] A. Kouibia, M. Pasadas, Approximation of surfaces by fairness bicubic splines, Adv. Comput. Math. 20 (2004) 87–103, http://dx.doi.org/10.1023/A:1025805701726.
[17] J. Branch, F. Prieto, P. Boulanger, A hole-filling algorithm for triangular meshes using local radial basis function, in: Philippe P. Pébay (Ed.), Proceedings of the 15th International Meshing Roundtable IMR, Springer, 2006, pp. 411–431, http://dx.doi.org/10.1007/978-3-540-34958-7_24.
[18] J.C. Carr, et al., Reconstruction and representation of 3D objects with radial basis functions, in: SIGGRAPH'01 Proceedings of the 28th Annual Conference on Computers Graphics and Interactives Techniques, 2001, pp. 67–76, http://dx.doi.org/10.1145/383259.383266.
[19] A.M. Sajo-Castelli, M.A. Fortes, M. Raydan, Preconditioned conjugate gradient method for finding minimal energy surfaces on Powell–Sabin triangulations, J. Comput. Appl. Math. 268 (1) (2014) 34–55, http://dx.doi.org/10.1016/j.cam.2014.02.030.
[20] A. Bouhamidi, Error estimates in Sobolev spaces for interpolating thin plate splines under tension, J. Comput. Appl. Math. 200 (1) (2007) 208–216, http://dx.doi.org/10.1016/j.cam.2005.12.014.
[21] A. Bouhamidi, A. Le Méhauté, Radial basis functions under tension, J. Approx. Theory 127 (2) (2004) 135–154, http://dx.doi.org/10.1016/j.jat.2004.03.005.
[22] J. Duchon, Sur l'erreur d'interpolation des fonctions de plusieurs variables par les D^m-splines, ESAIM: Math. Model. Numer. Anal. - Modél. Math. Anal. Numér. 12 (4) (1978) 325–334, http://dx.doi.org/10.1051/m2an/1978120403251.
[23] R. Arcangéli, M.C. López de Silanes, J.J. Torrens, Multidimensional Minimizing Splines. Theory and Applications, Kluwer Academic Publishers, 2004.
[24] M.A. Fortes, P. González, A. Palomares, M.L. Rodríguez, Filling holes using a mesh of filled curves, Math. Comput. Simulation 164 (2019) 78–93, http://dx.doi.org/10.1016/j.matcom.2018.12.012.